species in $CDCl_3$ solution. We have further investigated this question by examining the ^{17}O NMR pH titration of the tetraethyl ester of PNP labeled in one nonesterified phosphoryl oxygen; the data are shown in Figure 15. Protonation of the monoanion is accompanied by an upfield change in chemical shift of 5.4 ppm; the pK_a obtained from these data is 4.21 ± 0.04, a value which is in fair agreement with that obtained by ^{31}P NMR pH titration and potentiometric titration.[6c] The change in chemical shift per charge neutralized for the labeled oxygen is 10.8 ppm, a value considerably smaller than that expected if protonation were occurring exclusively on the oxygen.[10,16] This chemical shift change may be interpreted as resulting from either a minor but significant contribution by the imino tautomer to the solution structure of the tetraethyl ester of PNP or resonance stabilization of the negative charge of the monoanion by charge delocalization on the phosphoryl oxygens. Even though we cannot unequivocally distinguish between these explanations, we believe that the small change in ^{15}N chemical shift observed upon protonation of the monoanion is a reasonably accurate reflection of the magnitude of the chemical shift change caused by charge neutralization of this type of nitrogen. This value, approximately 2.50 ppm, is considerably smaller than those documented for protonation of other types of nitrogen atoms.[20-22]

Summary

The ^{15}N and ^{17}O NMR studies reported in this article are consistent with proton binding to imidodiphosphates, including AMP-PNP, occurring only through interactions with the phosphoryl oxygens, with no participation by the nitrogen atom in the P–N–P bridge. Furthermore, our results indicate that AMP-PNP and PNP both exist in solution primarily as the imido tautomers. The NMR data described in this and our previous papers[10,16] provide an unambiguous characterization of the sites of proton binding in ATP and its widely used structural analogues. Finally, we have found that protonation of the nitrogen anion of the tetraethyl ester of PNP is accompanied by an unusually small change in the ^{15}N NMR chemical shift.

Note Added in Proof. The crystal structure of the tetraphenyl ester of imidodiphosphate was recently solved by Mr. Kent R. Myers and Professor Joseph R. Murdoch, University of California, Los Angeles. In the solid this imidodiphosphate ester exists as the imido tautomer, a result in keeping with the solution studies reported in this article. We are grateful to Mr. Myers and Professor Murdoch for allowing us to quote their results prior to publication.

Acknowledgment. We thank Dr. Vladimir Basus and Alan Koretsky for assistance with the NMR experiments at UCSF and Professor Sunney I. Chan and Dr. Luciano Mueller for their generous assistance in obtaining the 67.8-MHz ^{17}O NMR spectra. This research was supported by grants from the National Institutes of Health (AM-17323 to G.L.K., GM-22350 to J.A.G., and GM-22982 to N.J.O). The Varian XL-100 NMR spectrometer was purchased with a grant from the NIH Division of Research Resources (RR-00892-1A1). The high-field NMR spectrometers used in this research are supported by grants from the National Science Foundation (Bruker WH-270 in the Southern New England Regional NMR Facility, NSF CHE-791620, and Bruker WM-500 in the Southern California Regional NMR Facility, NSF CHE-7916324).

Registry No. [β,γ-^{15}N]-AMP-PNP, 86993-96-6; [α-$^{17}O_1$]-AMP-PNP, 86993-97-7; [β,γ-^{17}O]-AMP-PNP, 86993-98-8; [$^{17}O_1$]-AMP, 86993-99-9; Na_4[^{15}N]PNP, 81068-46-4; Et_4[^{15}N]PNP, 86993-90-0; Na_4[^{17}O]PNP, 86993-91-1; Et_4[^{17}O]PNP, 86993-92-2; [^{15}N]dichlorophosphoryltrichloroiminophosphorane, 50535-66-5; dichlorophosphoryltrichloroiminophosphorane, 13966-08-0; diethyl [^{17}O]phosphoramidate, 86993-93-3; diethyl chlorophosphite, 589-57-1; diethyl [^{17}O]phosphite, 86993-94-4; diethyl [^{17}O]phosphorochloridate, 86993-95-5.

(20) Markowski, V.; Sullivan, G. R.; Roberts, J. D. *J. Am. Chem. Soc.* **1977**, *99*, 714.
(21) Cain, A. H.; Sullivan, G. R.; Roberts, J. D. *J. Am. Chem. Soc.* **1977**, *99*, 6423.
(22) Bonner, F. T.; Degani, H.; Akhtar, M. J. *J. Am. Chem. Soc.* **1981**, *101*, 3739.

Electron Paramagnetic Crystallography of Cobalt(II) and Copper(II) Carboxypeptidase A

L. Charles Dickinson* and J. C. W. Chien*

Contribution from the Department of Chemistry and Materials Research Laboratories, University of Massachusetts, Amherst, Massachusetts 01003. *Received December 23, 1982*

Abstract: Electron paramagnetic resonance spectra of single crystals of cobalt(II) carboxypeptidase A (CoCPA) and copper(II) carboxypeptidase A (CuCPA) have been obtained and solved for the orientation of the principal values of the ***g*** and hyperfine (***A***) tensors. The largest *g* and *A* canonical values for both species are found to be near the perpendicular to the plane containing the His-196 and 69δ-histidine nitrogen atoms and the metal ion. Further, the orientation of the three respective components of the ***g*** tensors of the CoCPA and CuCPA deviates no more than 30° from being parallel. This is taken to indicate that the distortions of the ligand fields in CuCPA and CoCPA are similar in their influence upon the d orbitals, each of which is at least half-filled in both copper(II) and high-spin cobalt(II). The copper hyperfine tensor is precisely parallel to the ***g*** tensor in CuCPA, and the splitting pattern in CuCPA is consistent with two equivalent nitrogen atoms. Cobalt hyperfine splitting is seen only along the direction of the maximum *g* value in CoCPA. The presence of "extra" sites in the CoCPA crystals suggests that conformational substates or ligand variations are possible. The two important results are that the ligand field strongly influences the directions of the ***g*** and ***A*** tensors, which are nearly the same for the d^7 CoCPA and the d^9 CuCPA. Secondly, the lack of enzyme activity in CuCPA may be related to the absence or inaccessibility of conformational substates.

Electron paramagnetic resonance (EPR) spectra have been employed for structural determination of metal sites and spin-labels in metalloenzymes and metal ion activated enzymes over the past 25 years. However, the bulk of these studies have involved frozen solution spectra that are ambiguous, especially when there is considerable electron density on the ligands. Many assignments of principal values for ***g*** and ***A*** tensors based on frozen solution data were shown to be wrong when single-crystal EPR results

0002-7863/83/1505-6481$01.50/0

became available.[1] A further advantage of single-crystal EPR is the ability of the technique to reveal more metal ion sites than predicted by X-ray crystallography. For instance, the spin-labels attached to β93-Cys in hemoglobin can assume two or many orientations depending upon the molecular size of the spin-label.[2] The oxygen ligands in oxycobaltomyoglobin[3,4] and the nitric oxide ligands in Hb Kansas[5] were found by single-crystal EPR to have two orientations. Many more orientations of the heme are possible in catalase[6] than are required by the X-ray crystallographic space group. These conformational substates reflect the ability of an enzyme molecule to make minor adjustments in its biological functions; the molecules do not have a rigid fixed structure.

Even though temperature-dependent X-ray crystallography[7] and Mössbauer spectroscopy[8] are being used to study conformational substates, single-crystal EPR is the tool of choice to probe this fluxional aspect in the vicinity of the metal ion vis-ã-vis X-ray crystallography and is more versatile than the Mössbauer technique. The central purpose of this work is to make a systematic investigation of the state of ligation and conformational substates of a metal-activated enzyme and to compare an active and an inactive metal-substituted species of the same protein.

The system chosen by us is carboxypeptidase A (CPA), which has been studied extensively by many chemical and physical techniques, most notably X-ray crystallography, which has resulted in a highly refined structure.[9] These details allow a number of deductions about the steps involved in peptide and ester cleavage.[10] This enzyme has long been known to be activated by Co(II), Ni(II), Mn(II), and Fe(II), with Co(II)CPA being a more active proleolytic enzyme than the native Zn(II)CPA, whereas CuCPA is inactive.[11] In the native Zn(II)CPA the Zn has a coordination number of five with the Nδ nitrogen atoms of histidines-69 and -196, both oxygen atoms of glutamate-72, and a water molecule in a quasi-tetrahedral array.[9] The water molecule is replaced by amino nitrogen and carbonyl oxygen donors in its substrate complexes. EPR crystallographic study of CoCPA and CuCPA would enhance the understanding of the distortions on the electronic structure by the ligand field and some measure of accessibility of conformational substates. Because of the unique distorted geometries found in CPA–metal complexes, the orientational results will also be of interest in studying low-symmetry EPR systems.[12]

Experimental Section

Carboxypeptidase A was purchased from Sigma Chemical Co. in two forms. Type I CPA(Cox), which has been used for most of the published X-ray crystallographic work, did not form crystals of sufficient size for EPR. Type II crystals of up to 2 mm on a side were grown by the following procedure. One milliliter of 25 mg/mL CPA was placed in a 2 × 0.5 cm dialysis bag and dialyzed against the series of 1,10-phenanthroline and NaCl buffers prescribed by Latt and Vallee.[13] All buffers were passed through a bed of fresh Chelex 100 ion-exchange resin to remove trace metals. All vessels were polyethylene washed with concentrated HNO_3 and deionized water. The dialysis bag and contents were then treated with sodium acetate (NaOAc) buffers of concentration decreasing in 0.05 M steps at 24-h intervals beginning with 0.6 M NaOAc. At 0.25 NaOAc small crystals were evident and the dialysis bag was allowed to sit undisturbed for 5 days as the crystals grew larger. There were about 10 nucleation sites per dialysis bag. X-ray analysis was performed on these apocrystals. A buffer 0.20 M in NaOAc or 10^{-4} M in $Co(OAc)_2$ or $Cu(OAc)_2$ or $^{65}Cu(OAc)_2$ was used to diffuse metal ions into the apocrystals. In Co buffer, these crystals turned from colorless to a faint purple after several days of exposure to excess buffer. The $Co(OAc)_2$ was prepared from high-purity metal (Alfa-Ventron, Puratronic Grade). $Cu(OAc)_2$ was A.C.S. Certified Grade from Fisher Scientific Co. ^{65}Cu was purchased from Oak Ridge National Laboratories, Oak Ridge, TN, digested in HCl, and diluted with $NaAc_2$ buffer. Cu-exposed crystals were very faint blue in color.

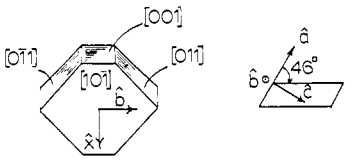

Figure 1. Sketch of habit of CPA crystals grown by the method described in the text showing major faces and cross section through the *zx* (*ac*) plane.

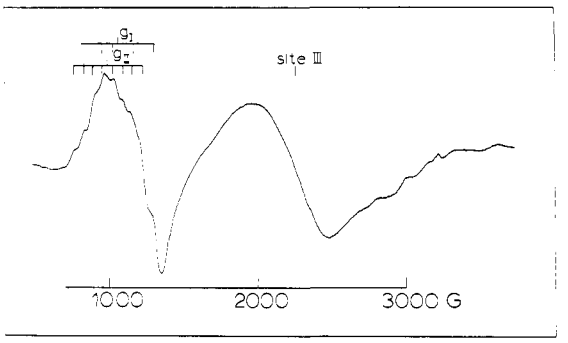

Figure 2. EPR spectrum of single-crystal CoCPA near the *b* axis showing the two types of sites. Modulation, 10 G; gain, 5 × 10^3; 30-mW microwave power; 10 K; 9.292 GHz.

Precession diffraction patterns at a 6-cm film-to-crystal distance were obtained from a well-formed crystal, giving identification of the major crystal faces as shown in Figure 1. Unit cell dimensions *a*, *b*, *c*, and β were 52.9 Å, 60.7 Å, 45.8 Å, and 97.25°.

EPR spectra were recorded on a Varian E-9 spectrometer fitted with a Helitran LTD-110 helium cryostat. The goniometer and crystal mounting system have been previously described.[14] Data analysis and computer processing were as previously described.[1] Temperature calibration was referred to liquid helium and liquid nitrogen with assumption of linear interpolation.

EPR crystallographic data were taken in planes conveniently related to the dominant face of the habit, 10$\bar{1}$, and an axis system was constructed with *z* perpendicular to that face and $x \perp z$ and *b*. Thus, the *xb*, *bz*, and *zx* planes were the observational planes, and by simple rotation matrix multiplication the data in the observed frame could be related to the crystallographic axes or any axis system of choice.

Results

Figure 2 shows an EPR spectrum of CoCPA at 4 K, with the magnetic field direction near the *b* axis direction in the *bz* plane. Sites I and II belong to the oriented cobalt species described in this paper. Site III also varies in position as the crystal is turned but could not be detected in other planes so no orientation information could be derived for site III. The hyperfine splitting into eight lines [$I(^{59}Co) = {}^7/_2$] is seen only within ±15° of the *b* axis and in that region sites I and II overlap severely, limiting the accuracy of determination of hyperfine variation with angle and the relative alignment of the *g* and *A* (Co) tensors. Variations of the *g'* factor with angle for the *xb* and *zx* planes are shown in Figure 3 along with computer-fitted lines. The *zx* plane corresponds to the *ac* crystallographic plane, so according to the $P2_1$ crystallographic symmetry, sites I and II become equivalent. In the *bz* plane because of the overlap of sites I and II in the region

(1) Dickinson, L. C.; Chien, J. C. W. In "Biological Magnetic Resonance"; Berliner, L.; Reuben, J., Eds.; Plenum Press: New York, 1981; Vol. III, pp 155–211.
(2) Chien, J. C. W. *J. Mol. Biol.* **1979**, *133*, 385.
(3) Chien, J. C. W.; Dickinson, L. C. *Proc. Natl. Acad. Sci. U.S.A.* **1972**, *69*, 2783.
(4) Dickinson, L. C.; Chien, J. C. W. *Proc. Natl. Acad. Sci. U.S.A.* **1980**, *77*, 1235.
(5) Dickinson, L. C.; Chien, J. C. W. *J. Biol. Chem.* **1977**, *252*, 133.
(6) Dickinson, L. C.; Chien, J. C. W.; Marie, A. L.; Parak, F. *Proc. Natl. Acad. Sci. U.S.A.* **1982**, *79*, 7278.
(7) Frauenfelder, H.; Petsko, G. A.; Tsernoglou, D. *Nature (London)* **1979**, *280*, 558.
(8) Parak, F.; Knapp, E. W.; Kucheida, D. *J. Mol. Biol.* **1982**, in press.
(9) Rees, D. C.; Lewis, M.; Honzatko, R. B.; Lipscomb, W. N.; Hardman, K. D. *Proc. Natl. Acad. Sci. U.S.A.* **1981**, *78*, 3408.
(10) Lipscomb, W. N. *Proc. Natl. Acad. Sci. U.S.A.* **1980**, *77*, 3875.
(11) Coleman, J. E.; Vallee, B. L. *J. Biol. Chem.* **1960**, *235*, 390.
(12) Pilbrow, J. R.; Lowrey, M. R. *Rep. Prog. Phys.* **1980**, *43*, 4269.
(13) Latt, S. A.; Vallee, B. J. *Biochemistry* **1971**, *10*, 4263.
(14) Dickinson, L. C.; Chien, J. C. W. *J. Am. Chem. Soc.* **1971**, *93*, 5036.

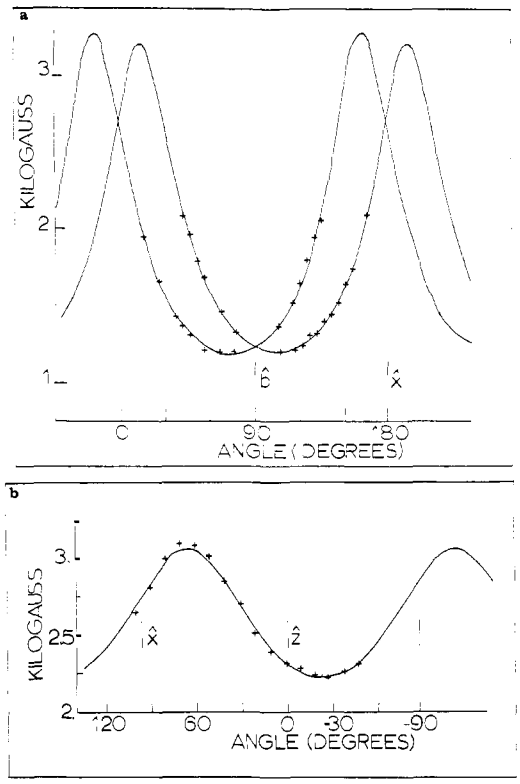

Figure 3. Field dependence of EPR resonance positions for the (a) *xb* and (b) *zx* planes. Points are observed positions; solid lines are computer fitted. For the *xb* case each site was fitted independently.

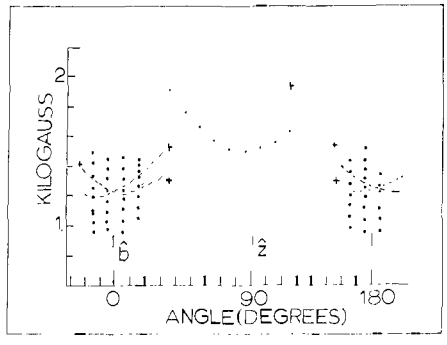

Figure 4. Field dependence of EPR spectra in the *bz* plane of CoCPA crystals. Data could not be computer fitted and were processed as described in the text.

near *b* and the obscuring effect of site III, it is not possible to assign sufficient line positions to successfully computer fit the data for that plane. In lieu of that accuracy, the components of the $(g')^2$ matrix in the *xbz* frame for the *bz* plane were computed from g'_+ and θ_+ (observed), and $g' \simeq 2.9$ estimated from the *xz* plane data from Schonland's equation,[15] where the subscript + (−) refers to maxima (minima) in a given plane. The observed data are shown in Figure 4 for the *bz* plane. Because of relatively small inconsistencies in the redundantly determined elements of the $(g')^2$ matrix in the *xbz* frame, the values were averaged. The uncertainty in this procedure causes no significant error in the g' value near 6 but a variation of about ±0.1 in the g' values near 2. The corresponding shifts in directions of principal values are ±2° and ±10°.

The eigenvalues and eigenvectors for the cobalt sites are shown in Table I. Because several crystals were used, there is the usual ambiguity in the signs of the off-diagonal elements in the g' matrix in the *xbz* frame. This ambiguity is, however, readily eradicated because for one choice of sign the resulting eigenvalues deviate significantly from the frozen solution values.

(15) Schonland, D. S. *Proc. Phys. Soc., London* **1959**, *73*, 788.

Table I. EPR Parameters from Single Crystals of Cobalt Carboxypeptidase

	eigenvector component (corresponding angle) for g value		
	2.13	2.64	6.65[a]
a	−0.530 (122)	0.799 (37)	0.279 (74)
b	±0.106 (83, 97)	±0.264 (105, 75)	±0.959 (17, 163)
c[a]	0.840 (32)	0.535 (57)	0.056 (87)

[a] ^{59}Co hyperfine splitting of 80 G was resolved near $g = 6.65$ ($A = 2.48 \times 10^{-2}$ cm^{-1}).

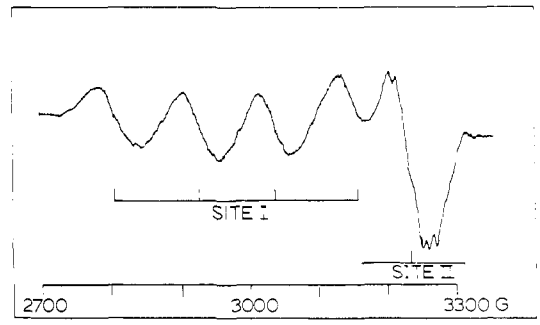

Figure 5. EPR spectrum of a single crystal of ^{65}CuCPA in the *bz* plane with H_0 along the bisector of *b* and *z*. Gain, 2.5×10^3; modulation, 4 G; power, 10 mW; 9.35 GHz.

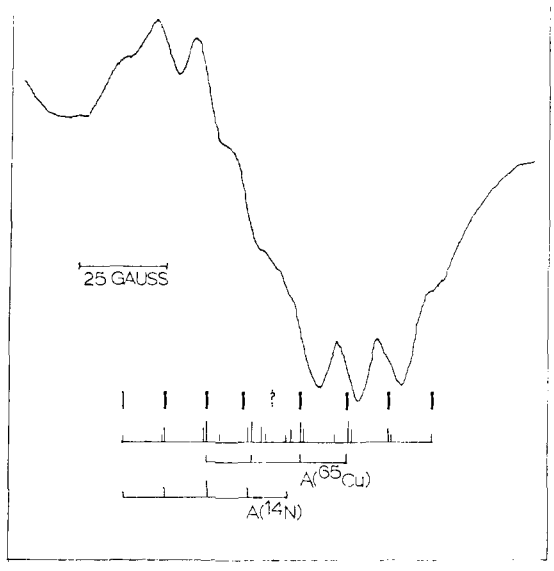

Figure 6. EPR spectrum of sample oriented as in Figure 5 but with an expanded scale showing detailed hyperfine splitting. The same instrumental settings as in Figure 5 were used for gain = 1.25×10^4 and field axis expansion.

The EPR signal of CoCPA was found not to saturate at the maximum available klystron power of 200 mV. The signal intensity, but not the shape, was found to change as the temperature was raised from 4 K and disappeared at 25 K.

CuCPA. An EPR spectrum of ^{65}CuCPA with the magnetic field in the *bz* plane, approximately 45° between *b* and *z*, is shown in Figure 5. Two sites are seen as expected for the $P2_1$ space group. At this orientation the two signals from the two sites are free from overlap interferences, and an expanded scale spectrum of the high-field site is shown in Figure 6, which allows the deduction that the splitting results from two equivalent nitrogen nuclei and approximately equal splitting from the ^{65}Cu($I = {}^3/_2$) nucleus.

Variation of *g* values and *A*(Cu) values were followed over the *xb*, *bz*, and *zx* planes and computer fitted as described above. The results are shown in Figure 7. The *g* and *A*(Cu) values have identical turning points, indicating that the two tensors are identically oriented with respect to the molecular frame. Principal

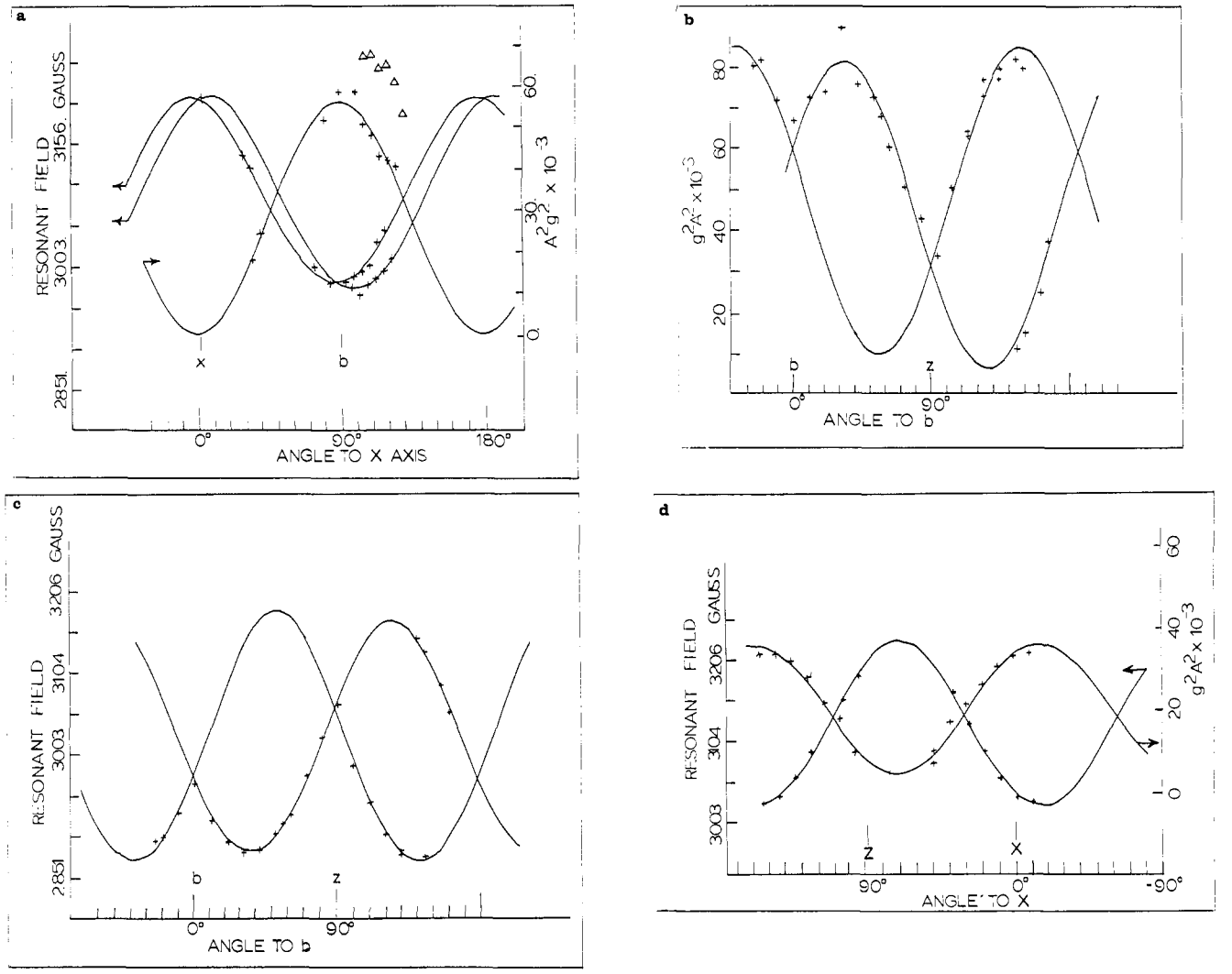

Figure 7. Variation of hyperfine splitting single-crystal CuCPA with angles in the (a) *xb*, (b, c) *bz*, and (d) *zx* planes. The solid lines are computer fittings to Schonland's equation.[15] The triangles show observed line positions that could not be fitted.

Table II. EPR Parameters from Single Crystals of Copper(II) Carboxypeptidase

	eigenvector component (arcosine) for *g* eigenvalue		
	2.04_2	2.10_9	2.31_4
a	−0.1962 (101)	−0.7988 (143)	+0.5679 (55)
b	±0.2122 (102, 78)	±0.6004 (53)	±0.7710 (40, 140)
c[a]	0.95681 (17)	−0.0308 (92)	+0.2874 (73)

	eigenvector component (arcosine) for *A*(Cu) eigenvalue		
	a	47.1×10^{-4} cm^{-1} (47.9 G)	135.4×10^{-4} cm^{-1} (125.4 G)
a	−0.1554 (99)	−0.8404 (147)	+0.5184 (59)
b	±0.2316 (103, 77)	±0.5414 (57, 123)	±0.8082 (36, 144)
c[a]	0.9599 (16)	−0.0044 (90)	+0.2788 (74)

[a] The lowest eigenvalue was negative (−8 G) upon diagonalization. Varying the original A^2g^2 matrix so that zero or small positive values resulted had little effect on the direction cosines or other eigenvalues.

values and direction cosines (angles) are presented in Table II. The eigenvalues for both ***g*** and ***A*** show wide deviation from axial symmetry. An attempt was made to fit the data of hyperfine variation in CuCPA with a modified Schonland's equation with addition of a $\delta \sin(2\theta) \cos(2\theta)$ term; no improvement in the fitting resulted.

Discussion

The geometric alignment of the electronic structure and its properties such as the ***g*** and ***A*** tensors is of great interest in metal-replaced enzymes because the ligand environments of the metal are known to deviate widely from ideal symmetry. However, as the symmetry is reduced to C_{2h} or lower, a number of difficulties arise[12] both in determining the true parameters of the Hamiltonian and in computing models that give molecular meaning—spin densities, orbital splittings, etc.—to the data. For high-spin Co(II) we have the additional complication that the zero-field splitting tensor for the three unpaired electrons increases the number of unknown parameters well beyond the number of observable parameters.[16] Although theory has not progressed to the level of reducing the observed rhombic tensor elements to molecular properties, the comparative observations presented here do show striking similarities in CoCPA and CuCPA that will hopefully stimulate further work by theoreticians.

In order to discuss the directional information, we construct a stereographic projection of the directions of principal *g* values in a frame determined by the coordinates of the zinc enzyme as determined by Lipscomb.[17] While there are no assurances that ligand atoms on the zinc enzyme will retain their exact location in the metal-replaced enzyme, it seems reasonable to assume that the approximate locations of, for example, the nitrogen atoms will be conserved. We thus construct a coordinate (vector) system with $\mathbf{N}_1 = \mathrm{N}_\delta$(His-69)–Zn; $\mathbf{N}_2 \perp \mathbf{N}_1$ in the N_δ(His-69)–Zn–N_δ(His-96) plane, and $\mathbf{N}_1 = \mathbf{N}_1 \times \mathbf{N}_2$. $\mathbf{N}_1$ thus points approximately along the direction of the Zn–H_2O bond.

(16) Banci, L.; Bencini, A.; Benelli, C.; Gatteschi, E. *Nouv. J. Chim.* **1980**, *4*, 593.
(17) Lipscomb, W. N.; Shoham, G., personal communication.

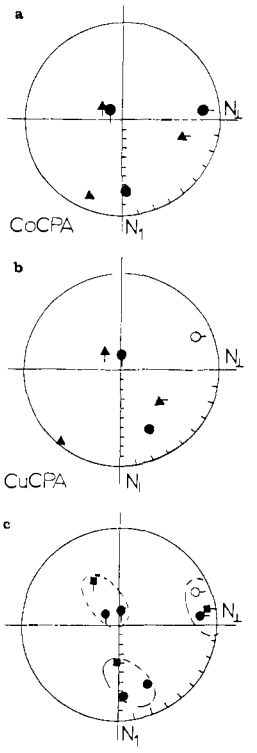

Figure 8. Stereographic projection of directions of principal g tensor eigenvectors onto the ZnCPA-determined (N_1, $N_\perp$, N_2) coordinate system described in the text for (a) CoCPA, (b) CuCPA, and (c) preferred assignments for both CuCPA and CoCPA. (●) Preferred assignment; (▲) alternative assignment; (■) shift directions for CoCPA within a reasonable range of variation of indeterminate parameters in the *bz* plane. The maximum (mininum) g value is denoted by a tick mark on right (bottom) side of the symbol. Unfilled symbol (○) denotes projection from below the plane.

Figure 8 shows stereographic projections[18] of the principal directions of the principal g tensor components onto the above coordinate system for CuCPA and CoCPA.

Because we observe at least two sites for each species, there is 2-fold ambiguity as to which site can be correctly assigned to the coordinate system. We have depicted both possibilities in the projections although there is some reason for a preferred assignment as discussed below. Figure 8c shows the preferred direction assignment for both CoCPA and CuCPA in the same stereogram. Because of the insufficiency of data for computer fitting in the *bz* plane described above, the CoCPA case has a range of indeterminacy. The two ways of estimation of the inaccurately known components to the $(g')^2$ $(\hat{x}, \hat{b}, \hat{z})$ matrix give the two possibilities shown in Figure 8c for CoCPA. The angles between the directions of g_{max}, g_{int}, and g_{min} for the CuCPA and CoCPA can be readily computed to be 23°, 35°, and 29° for the first CoCPA assignment and 24°, 19°, and 14° for the second. These numbers are remarkably small with respect to the possible maximum of 90° if the CoCPA and CuCPA directions were uncorrelated. Thus, it appears that the directions and relative g values of tensor components for CuCPA and CoCPA are determined by similar structural factors. As Co(II) is a d^7 high-spin system, and Cu(II) is a d^9 one-spin system, this result is surprising. As the CoCPA g' values are effective g values dominated by zero-field splitting and the CuCPA g values are for a one-electron case, it is even more surprising to see this orientation correlation between the two metal-replaced species.

A qualitative understanding of this correlation may be obtained by considering that for high-spin Co(II), regardless of what one considers to be the ground state, all five d orbitals have at least one unpaired electron. This is also true for Cu(II). While the detailed theory of $\boldsymbol{g}$ and $\boldsymbol{D}$ tensors would be formidable to work out under such a low-symmetry ligand field as is known for ZnCPA, it is recognized that there is a relationship between the formalism for the $\boldsymbol{g}$ and $\boldsymbol{D}$ tensors on the general level[18] that would make it plausible for the $\boldsymbol{g}$ and $\boldsymbol{D}$ tensors to have the same orientation, although considerations for large $\boldsymbol{D}$ in a pseudotetrahedral complex place $\boldsymbol{g}$ and $\boldsymbol{D}$ nonparallel.[19] For CoCPA we expect $\boldsymbol{D}$ to be low as described later, and the direction of the effective $\boldsymbol{g}'$ tensor must be governed by the $\boldsymbol{g}$ tensor alone. Theoretical $\boldsymbol{g}$ tensor expressions are of the form

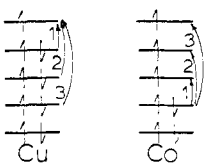

Figure 9. Schematic of hypothetical energy level and electron configuration for Co and Cu used to rationalize correlation between $\boldsymbol{g}$ tensor orientation in CoCPA and CuCPA.

$$\boldsymbol{g}_i = 2.0023 + 2\lambda\sum_n \frac{\langle 0|L_i|n\rangle\langle n|L_z|0\rangle}{E_0 - E_n} \qquad (1)$$

where $i = x$, y, or z, λ is the spin–orbit coupling constant (negative for d^7 and d^9 configurations), L_i is an angular momentum operator, 0 (n) indexes the ground- (excited-) state wave function, and E_n is the energy of the nth state. In Figure 9 is a schematic level diagram for d orbitals in the field of the "CPA" ligands. The terms in eq 1 are governed by symmetry and spacing. Clearly if orbitals n and 0 cannot mix, by symmetry, then $\langle 0|L_i|n\rangle$ becomes zero. However, as the ligand symmetry is lowered, the restrictions on symmetry become relaxed and more terms become nonzero. We consider the extreme case of all possible d transitions that do not change the spin multiplicity in Figure 9. Under this relaxed, hypothetical setup, one can see that the same orbitals will contribute to terms in eq 1 for a given term, L_i. Thus, if the same orbitals contribute under the same symmetry, the directions of the principal values will be the same, though the values will be scaled by λ, and the contribution of each term will be weighted by $(E_0 - E_n)^{-1}$. In this light, it is not remarkable that the $\boldsymbol{g}$ tensors for Cu and Co have the same orientation, but it is surprising that the alignment of the $\boldsymbol{g}$ tensors also have g_{min}, g_{int}, and g_{max} in correspondence. This undoubtedly implies a relationship between the spacing of the d orbitals. If the allowed transition for a given canonical direction are, say, as in Figure 9, the leading term as far as $(E_0 - E_1)^{-1}$ weighting goes will be different for Co and Cu. This difference is somehow compensated in keeping g_{max}, g_{int}, and g_{min} in the same direction in CoCPA and CuCPA.

CuCPA. The rhombic components of the $\boldsymbol{g}$ and $\boldsymbol{A}$ tensors for CuCPA indicate a strongly asymmetric ligand field of the copper ion in the protein environment. If the ligand field in CuCPA is closely related to that of the ZnCPA as found by X-ray crystallography, the arrangement is roughly tetrahedral but with one of the tetrahedral directions occupied by two off-axis oxygen atoms of the carboxyl group of Glu-72. The deviation of EPR parameters from axial symmetry is large compared to that previously reported from frozen solution CuCPA.[20] Failure of these authors to observe the g_{int} line apparently resulted from fortuitous overlap in the high-field region. It is also possible that the difference results from buffer composition. The above authors explored, by means of a series of copper complexes that had been studied by X-ray crystallography, electronic spectroscopy, and frozen solution EPR, the variation of $g_\parallel$ and $A_\parallel$ with the degree of distortion from a square-planar toward a tetrahedral array of ligands. They concluded on this basis that CuCPA had a pseudotetrahedral array of ligands. While this picture of the ligation seems certain, the rhombic tensors observed by us strongly suggest that further details of the distortion are contained in the EPR information. Although

(18) McGarvey, B. R. In "Transition Metal Chemistry"; Carlin, R. L., Ed.; Marcel Dekker; New York, 1966; Vol. 3, p 116–118.

(19) Bencini, A.; Gatteschi, D. *Inorg. Chem.* **1977**, *16*, 2141.

(20) Rosenberg, R. C.; Root, C. A.; Bernstein, P. K.; Gray, H. B. *J. Am. Chem. Soc.* **1975**, *97*, 2092.

tetrahedral Cu(II) complexes have been studied extensively[21] in both theory and observation, the high symmetry compared to our case make these studies of very limited use. However, isotropic g and A tensors are not observed even in these cases. Recent interest in low-symmetry copper complexes has centered on deviations of the x and y components from expected angles with respect to ligand directions for C_2, C_{2h}, and C_s symmetry,[22,12] but to our knowledge the further complication of deviation of $g_\parallel$ from the normal to the strong ligand plane has not been treated.

Low-symmetry effects on EPR spectra show up as deviations from coincidence between g and A tensors and as deviations of dependence of observed g or A values in a given plane from simple sinusoidal curves. The obvious systematic deviation of residuals in fitting g^2A^2 (Figure 7b,c) to the simple sinusoidal function may reflect some low-symmetry effects. In Figure 7c g^2A^2 for one site could not be fitted at all, yet the other site fit fairly well. The coincidence of orientation of the g and A tensors for CuCPA is somewhat surprising as low-symmetry effects generally cause noncoincidence.

The expanded spectrum of ^{65}CuCPA in Figure 6 shows some irregularity in spacing and resolution. At this orientation it is clear that there is no interference from the other sites in the crystal. Eight lines are unambiguously resolved, but the intensities are obviously affected by overlap. The most likely possibility for hyperfine splitting in the spectrum from a CuN_2 moiety is near-equivalent splitting constants for the copper and nitrogen nuclei. In other words, one observes a quartet from Cu($I = {}^3/_2$) of overlapping 1:2:3:2:1 quintets (from two equivalent $I = 1$ nuclei) with the result as a 1:3:6:8:8:6:3:1 octet. The peak height pattern does not show these extremes, but a slight inequivalence (less than the line width) among the Cu and N splitting constants involved would decrease the effective heights from those of the idealized pattern. There is a previous note on the observed equivalence of nitrogen splitting in CuCPA single crystals.[23]

As mentioned above, there are two ways of assigning the principal g tensor directions to the N_1, N_1, N_2 coordinate system. The N_1N_2 plane is that of the stronger, nitrogen ligands so that N_1 should correspond to the direction of the largest g value in much the same way as it would for a typical square-planar complex. Although it is apparent that our complex has deviations of g_{max} from the N_1 direction, it is a reasonable assumption to make the coordinate system assignment on the basis that the one placing g_{max} nearer to N_1 is the correct one.

CoCPA. It is also impossible to rigorously select the correct coordinate assignment for CoCPA, but there are some arguments based on model compounds that favor the choice of the direction of the maximum g' value nearly perpendicular to the plane of the nitrogen atoms, i.e., along N_1. Bencini et al.[24] have studied the pseudotetrahedral $CoCl_2O_2$ complex and found the maximum g' value to lie perpendicular the plane of the stronger, Cl, ligands. This choice places the smallest g'' value direction near the plane of the two nitrogen atoms approximately along their bisector; the intermediate g' value lies almost along the line connecting the two nitrogens.

A previous report on frozen solution EPR spectra of CoCPA[25] gives g' values of 5.7, 4.0, and 2.2 with no observable ^{59}Co hyperfine splitting. The buffer conditions are unspecified but are inferred to be NaCl–Tris rather than the acetate–Tris buffer used here. If the EPR parameters change with buffer, then they are more sensitive than are the optical spectra.[13] Such an EPR sensitivity was found in the case of cobalt carbonic anhydrase,[25] which has a metal binding site somewhat similar to that of CPA. The most probable site for ligation changes with buffer would be at the position of the bound water.

The reduction of EPR parameters for high-spin Co(II) to molecular parameters is complicated by the fine structure interactions between the three unpaired electrons. The observed g' values then become functions of the molecular g values as well as the two components of the fine structure tensor, $|D|$ and $|E|$. With three observed g_i' values (g_x, g_y, g_z, $|D|$, $|E|$) it is not possible to solve for all the unknowns,[26] so the usual assumption of axial symmetry, $g_x = g_y$, is made and only the ratio E/D is solved for. Depending on the sign of $|D|$, the $|\pm{}^1/_2\rangle$ or $|\pm{}^3/_2\rangle$ Kramers doublet may lie lowest and as $|E|$ deviates from 0 the two spin states mix and $^1/_2$ and $^3/_2$ become fictitious quantum numbers. The assumption of axial symmetry seems inappropriate for the low-symmetry CoCPA but necessary if any analysis is to be performed. With the equations of Pilbrow,[24] reduced to first order and with the above assumptions, for the $|\pm{}^1/_2\rangle$ ground state, one obtains $E/D \simeq 0.325$ and $g_\parallel = 2.0$ and $g_1 = 2.25$, which shows that the molecular g values are in a reasonable range.

There has been a great deal of theoretical effort expended on the theory of low-symmetry, high-spin cobalt(II) systems (see ref 16 and references cited therein). However, none even approximate the asymmetric site of the metal ion in carboxypeptidase. Most of the model computations achieve asymmetry by placing different atomic species at points on an ideal geometry, e.g., N_2O_2, tetrahedron; N_2O_3, trigonal bipyramid. The ZnCPA coordination described above fits none of the model systems calculated, and because of the deviations from ideal symmetry the underdetermined equations of the models are useless here.

The observation that the signal does not saturate at 4 K with high microwave power is surprising in comparison with other cobalt(II)-replaced enzymes. Recently, an EPR study of frozen solutions of cobalt liver alcohol dehydrogenase, Co(II)LADH, which has a coordination sphere of S_2NO,[28] employed the change in power for half-saturation with temperatures between 4 and 10 K to determine the zero-field splitting. The inability to saturate CoCPA at 4 K could imply that $2|D|$ would be considerably smaller than the 9.4 cm^{-1} determined for Co(II)LADH.

At the maximum g' value the individual line width is about 25 G; the smallest line width for an unresolved hyperfine line shape envelope is about 200 G near $g' = 4.4$ in the *bz* plane. The lines broaden to about 400 G in the *ac* plane, while g' is in the range 2–3. While it is impossible to separate effects on the line width from unresolved splitting and from distribution of alignments of the metal complex, the changes are less dramatic than for the heme proteins.[29] These heme proteins have g' anisotropy approximately the same as for Co(II)CPA yet a ±2° misalignment distribution of the heme or protein moiety causes the line width to vary from 50 to 800 G in metmyoglobin.

The clear appearance of more than two sites in the data for the *bz* plane is of great interest. As the X-ray crystallography confirmed the $P2_1$ space group and gave no evidence for twinning in this habit, this clearly means more than one metal coordination species is present in CoCPA under the buffer and freezing conditions we employ. As a *caveat* to the following discussion we note that other workers on X-ray crystallography[31] have observed in 0.01 M $CoCl_2$ two extra metal binding sites for CPA. There is precedent for freezing effects causing a heterogeneity in the geometry of a metal complex[30] in the case of oxycobaltomyoglobin. Two electronically inequivalent sites were generated below 243

(21) (a) Bates, C. A.; Moore, W. S.; Standley, K. J.; Stevens, K. W. H. *Proc. Phys. Soc., London* **1962**, *79*, 73. (b) Sharnoff, M. *J. Chem. Phys.* **1965**, *42*, 3383. (c) Parker, I. H. *J. Phys. C* **1971**, *4*, 2967.
(22) Belford, R. L.; Harrowfield, B.; Pilbrow, J. R. *J. Magn. Reson.* **1977**, *28*, 433.
(23) Brill, A. S.; Kirkpatrick, R. P.; Scholes, C. P. In "Probes of Structure and Function of Macromolecules and Membranes"; Chance, B.; Lee, C. R.; Blaisie, J. R., Eds.; Academic Press: New York, 1971; Vol. I.
(24) Bencini, A.; Benelli, C.; Gatteschi, D.; Zancini, C. *Inorg. Chem.* **1979**, *18*, 2137.
(25) Kennedy, F. S.; Hill, H. A. O.; Kaden, T. A.; Vallee, B. L. *Biochem. Biophys. Res. Commun.* **1973**, *48*, 1533.
(26) Bencini, A.; Bertini, I.; Conti, G.; Gatteschi, D.; Luchinat, C. *J. Inorg. Biochem.* **1981**, *14*, 8193.
(27) Pilbrow, J. R. *J. Magn. Reson.* **1978**, *31*, 479.
(28) Makinen, M.; Yim, M. B. *Proc. Natl. Acad. Sci. U.S.A* **1981**, *78*, 6221.
(29) Helcke, G. A.; Ingram, D. J. E.; Slade, E. F. *Proc. R. Soc. London, Ser. B* **1968**, *169*, 275.
(30) Mori, M.; Ideda-Saito, M.; Yonetani, J. *J. Biol. Chem.* **1982**, *257*, 3636.
(31) Lipscomb, W. N.; Hartsuck, J. A.; Recke, G. N., Jr.; Quiocho, F. A.; Bethge, P. A.; Ludwig, M. L.; Steitz, T. A.; Muirhead, H.; Coppola, J. C. *Brookhaven Symp. Biol.* **1968**, *21*, 48.

°C giving distinct EPR spectra that were attributed to water structure changes upon freezing. The presence of two differently oriented oxygen ligands in crystals of this molecule at 77 K and their equilibration to one species at 125 K has already been cited.[4] Therefore, a more general statement is that there exist conformational substates of the protein and that freezing traps the molecule in two minima of nearly equal energy. In our CoCPA data, the appearance of the second feature would require some rearrangement of ligands. For the second site, the g value in the direction corresponding to $g = 2.0$ for the first complex is about 4.4. We note that CuCPA is devoid of esterase and peptidase activity whereas CoCPA is active. The absence of extra sites in the single crystals of CuCPA may be related to an inability of the metal complex to rearrange to accommodate substrates in a way that can be done by CoCPA. The inactivity of CuCPA may of course be related to a number of other "inappropriate" ligation properties of Cu. Our results suggest that a temperature-dependent study of the X-ray crystallography of CoCPA and ZnCPA would show a dynamism of the metal coordination sphere and related protein structural changes.

Acknowledgment. We are grateful to Professor J. S. Wood for discussions and for obtaining the precession photographs.

Registry No. Carboxypeptidase A, 11075-17-5.

Communications to the Editor

Reaction of Carbethoxycarbene with *o*-Carborane[1]

Guo-xiu Zheng[2] and Maitland Jones, Jr.*

Department of Chemistry, Princeton University
Princeton, New Jersey 08544

Received March 23, 1983

Nearly a century ago, Buchner and Curtius examined the thermal decomposition of ethyl diazoacetate in benzene.[3] It took much of the next hundred years to unravel the structures of the "Buchner esters".[4] It is now known that reaction of carbenes with benzene and other aromatic compounds proceeds by initial formation of the bicyclo[4.1.0] system (norcaradiene) which usually,[5] but not always,[6] opens to the related cycloheptatriene. The addition products are accompanied by smaller amounts of the products of carbon-hydrogen insertion. Methylene gives 9% toluene and 32% cycloheptatriene in its reaction with benzene.[7] Other carbenes give insertion products, but some of these compounds may be formed by rearrangements of norcaradienes.[8]

Benzene has a set of three-dimensional aromatic cousins in the icosahedral carboranes of which **1**, *o*-carborane, is the most accessible. Molecular orbital treatments yield a set of 13 bonding MO's, which are nicely filled by the available 26 electrons. Alternatively, **1** may be viewed as a combination of two caps and two five-membered rings.[9,10] A total of six electrons is contributed to "interstitial" bonding in the three-dimensionally aromatic system. Aromaticity is reflected in substantial thermal stability as well as traditionally "aromatic" chemical properties such as the ability to do aromatic substitution reactions.[11] Having already begun a study of the properties of divalent carbon attached to a carborane,[12] we wondered if carbenes would react with carboranes as they do with the "two-dimensionally" aromatic benzene. We chose to examine the generation of the well-studied carbethoxycarbene[5,13] with **1**.

Table I. Insertion of Carbethoxycarbene into the B-H Bonds of 1 vs. Calculated Framework Charges

	6	2	3	4	5
	C-H (1,2)	B-H (3,6)	B-H (4,5,7,11)	B-H (8,10)	B-H (9,12)
$h\nu$	0	4	19	29	47
Δ	0	3	19	27	52
Δ/CuCl	0	5	29	20	46
group charges[17]	+0.07	+0.03	0.00	−0.05	−0.05

Irradiation of ethyl diazoacetate in a hexafluorobenzene solution of **1** led to four products (**2–5**) (Scheme I), along with small amounts of ethyl fumarate, ethyl maleate, and, in the thermal reaction, hexafluorobenzene/carbene adducts. Separation of the four isomers was satisfactorily accomplished on a 6.5 ft × $^1/_4$ in. 15% QF-1 on 60/80 Chromosorb W column operated at 195 °C. Thermal decomposition of a hexafluorobenzene solution of **1** and ethyl diazoacetate in the presence or absence of CuCl led to the same four adducts. Table I gives the ratios as determined by gas chromatography, after reaction for 1 h.[14]

GC/MS showed that **2–5** incorporated the elements of the carbene and **1**. Precise mass spectrometry established the formulae as $C_6B_{10}H_{18}O_2$. ^1H NMR and infrared spectroscopy revealed that the ester function was retained, and ^{11}B NMR at 115.5 and 80.25 MHz permitted a detailed structural analysis.[15] The compounds

(1) Support of this work by the donors of the Petroleum Research Fund, administered by the American Chemical Society, and by the National Science Foundation (Grant CHE-81-01212) is gratefully acknowledged. Zheng, G.-x.; Sung, D. D.; Gallucci, R. R.; Chari, S. L.; Chiang, S.-H.; Jones, M., Jr. "Abstracts of Papers", 186th meeting of the American Chemical Society, Washington, D. C., Aug–Sept 1983, American Chemical Society: Washington, D.C., 1983; ORGN 0117.

(2) On leave from the Institute of Chemistry, Academia Sinica, Beijing, People's Republic of China.

(3) Buchner, E.; Curtius, T. *Ber. Dsch. Chem. Ges.* **1885**, *18*, 2377.

(4) Doering, W. von E.; Laber, G.; Vonderwahl, R.; Chaimberlain, N. F.; Williams, R. B. *J. Am. Chem. Soc.* **1956**, *78*, 5448.

(5) Kirmse, W. "Carbene Chemistry"; Academic Press: New York, 1971; Vol. 2.

(6) Ciganek, E. *J. Am. Chem. Soc.* **1967**, *89*, 1454.

(7) Doering, W. von E.; Knox, L. H. *J. Am. Chem. Soc.* **1953**, *75*, 297.

(8) Reference 5, p 227 ff.

(9) Jemmis, E. D. *J. Am. Chem. Soc.* **1982**, *104*, 7017.

(10) Jemmis, E. D.; Schleyer, P. v. R. *J. Am. Chem. Soc.* **1982**, *104*, 4781.

(11) (a) Grimes, R. N. "Carboranes"; Academic Press: New York, 1970. (b) Onak, T. "Organoborane Chemistry"; Academic Press: New York, 1975. (c) Beall, H. In "Boron Hydride Chemistry"; Muetterties, E. L., Ed.; Academic Press: New York, 1975; Chapter 9. For examples, see: Potenza, J. A.; Lipscomb, W. N. *Inorg. Chem.* **1966**, *5*, 1471, 1478, 1483 (*o*-carborane). Stanko, V. I.; Klimova, A. I.; Titova, N. S. *Zh. Obshch. Khim.* **1968**, *38*, 2817 (*m*-carborane).

(12) Chari, S. L.; Chiang, S.-H.; Jones, M., Jr. *J. Am. Chem. Soc.* **1982**, *104*, 3138.

(13) Jones, M., Jr., Moss, R. A., Eds. "Carbenes"; Wiley: New York, 1973; Vol. 1. Moss, R. A., Jones, M., Jr., Eds., "Carbenes"; Wiley: New York, 1975; Vol. 2.

(14) With time the insertion reaction apparently becomes more statistical. We are investigating the causes of this phenomenon and quote the $t = 1$ h data as our best approximation of the $t = 0$ h value. The yield of **2–5** is about 10% after 1 h and 20% after 40 h. Despite these modest yields the reaction is a useful one as the starting materials are simple and the products rather easy to isolate. At long reaction times GC/MS analysis shows small amounts of compounds formed from one carborane and two or even three carbenes.

(15) We are most grateful to Professor L. G. Sneddon of The University of Pennsylvania for help in obtaining the high-field ^{11}B spectra and for enlightening conversations about boron. Details of the analysis of spectra are available on request.

0002-7863/83/1505-6487$01.50/0